

Core-softened potentials and the anomalous properties of water

E. A. Jagla

The Abdus Salam International Centre for Theoretical Physics (ICTP), I-34014 Trieste, Italy

We study the phase diagram of a system of spherical particles interacting in three dimensions through a potential consisting of a strict hard core plus a linear repulsive shoulder at larger distances. The phase diagram (obtained numerically, and analytically in a limiting case) shows anomalous properties that are similar to those observed in water. Specifically, we find maxima of density and isothermal compressibility as a function of temperature, melting with volume contraction, and multiple stable crystalline structures. If in addition a long range attraction between the particles is included, the usual liquid-gas coexistence curve with its critical point is obtained. But more interestingly, a first order line in the metastable fluid branch of the phase diagram appears, ending in a new critical point, as it was suggested to occur in water. In this way the model provides a comprehensive, consistent and unified picture of most of the anomalous thermodynamical properties of water, showing that all of them can be qualitatively explained by the existence of two competing equilibrium values for the interparticle distance.

I. INTRODUCTION

Water is an anomalous substance in many respects.¹ Liquid water has a maximum as a function of temperature in both density and isothermal compressibility. It solidifies with volume increasing at low pressures, and the solid phase (ice) shows a remarkable variety of crystalline structures in different sectors of the pressure-temperature plane. Some of these properties are known from long ago, but their origin is still controversial. In an effort to rationalize these anomalous properties, the supercooled (metastable) sector of the phase diagram of liquid water has received much attention in the last years.²⁻⁶ It was observed that when appropriately cooled (using techniques for preventing crystallization) water becomes a viscous fluid with many properties (as heat capacity and isothermal compressibility) displaying a tendency that has suggested even a thermodynamic singularity at some lower temperature.⁷ Although there is a limit of about 235 K below which water cannot be cooled without crystallization, amorphous states of water at much lower temperatures can be obtained by different techniques. All these amorphous states are observed to correspond to one of two different structures (referred to as low-density amorphous -LDA- and high-density amorphous -HDA) that differ by about 20 per cent in density, which transform reversibly one into the other upon changes of pressure.⁸ There is evidence that these amorphous states are thermodynamically connected with fluid water, although a direct verification is not possible due to recrystallization at intermediate temperatures.⁹

The observation of LDA and HDA was an experimental clue that led to the proposal of the second critical point hypothesis.^{3,10,11} This hypothesis states that in the deeply supercooled region water can exist in two different amorphous configurations, separated by a line of first order transitions. This line should end in a criti-

cal point very much as the usual liquid-vapor line ends in a critical point. This hypothesis, in addition to obviously explain the reversible transformation between LDA and HDA, provides a natural though phenomenological explanation for the anomalous behavior of density and isothermal compressibility. However, the very existence of the second critical point is known to be not necessary for the appearance of other anomalies,^{12,13} and the issue of what are the microscopic properties of water molecules that may produce the appearance of the second critical point are only poorly understood. In all cases it seems to be crucial the fact that water (because of the particular form of its molecules and peculiarities of the hydrogen bond) exhibits competition between more expanded structures (preferred at low pressures) and more compact ones (which are favored at high pressures). But it is not obvious to what extent this simple fact can be made responsible for all the anomalies of water, or if more subtle properties of the interaction potential (in particular, cooperative hydrogen bonding)^{13,14} are crucial.

Numerical simulations based on some of the available pair potentials for the interaction between water molecules reproduce reasonably well many of its properties, although the systems that have been studied are strongly limited in size, due to computational constraints.^{15,16} These simulations only suggest the existence of the second critical point, but up to now they were not able to prove its existence unambiguously. Other simplified and in some cases ad-hoc models have been devised to show the appearance of anomalous properties in the phase diagram.¹⁷ Some of these models have a second critical point, but in these cases a global characterization of the phase diagram that includes all other anomalies has not been achieved. In all cases, the models used have as a fundamental ingredient the competition between expanded, less dense structures and compressed, more dense ones.

It is the goal of the present work to show that a very simple model of spherical particles interacting through a repulsive potential that possesses two different preferred equilibrium positions has a phase diagram in which a) lines of maxima for the density and the isothermal compressibility of the liquid exist; b) the fluid phase freezes with an increase in volume in some pressure range; c) the solid phase has multiple different crystalline structures depending on P and T . When a long range van der Waals attraction is included on top of the previous, exclusively repulsive potential, the system d) preserves the anomalies existent in the non-attractive case; e) develops a liquid gas first order coexisting line that ends in a critical point in the usual fashion; f) depending on the strength of the attractive potential, a line of first order transitions separating two amorphous phases in the supercooled region appears. This line ends in a second critical point from which the line of maxima in isothermal compressibility starts.

These statements will be justified mostly using numerical (Monte Carlo) techniques. However, for the deep supercooled states, the long equilibration times make the numerical studies not completely reliable. In this case, the numerical results are supported by analytical calculations in a limiting case of the interacting potential that shows neatly how the second critical point appears.

The paper is organized as follows. In Section II we give a brief description of the interaction potential and the numerical technique. Section III focus on the different stable crystalline configurations of the system. In Section IV we study the phase diagram of the fluid phase, both where it is thermodynamically stable and also in the supercooled region. Here we rely both in analytical calculations and in simulations, and show how a second critical point can appear. In Section V we describe the melting of the most expanded solid structure and its anomalies. Finally, in Section VI we take all the results as a whole and comment upon their importance for the understanding of the properties of water.

II. MODEL AND NUMERICAL DETAILS

The interaction potential $U(r)$ between particles that we will consider is chosen to be the hard-core plus linear-ramp potential originally studied by Stell and Hemmer.¹⁸ The radius of the hard core is taken to be r_0 , and the ramp extends linearly from the value ε_0 at $r = r_0$ up to 0 at $r = r_1$. In addition, a long range van der Waals attraction will be included through a global term in the energy per particle of the system proportional to $-\gamma/v$, with v the specific volume and γ a coefficient that represents the total integrated strength of the attraction. The van der Waals term can be accounted for without its explicit inclusion in the simulations in the following way.¹⁹ Since the free energy per particle contains the term $Pv - \gamma/v$, when minimizing with respect to v the combi-

nation $P + \gamma/v^2$ appears. So we will call $P^* \equiv P + \gamma/v^2$, and make the simulations in terms of P^* , with $\gamma = 0$. At the end, the self consistent replacement $P^* \rightarrow P + \gamma/v^2$ is made, and this provides the results for finite γ .

Numerical simulations are performed at constant P , T , and N (the number of particles) by standard Monte Carlo techniques. Periodic boundary conditions are used in the three directions. The equilibrium volume at each pressure is reached by allowing the system size to increase or decrease through Monte Carlo movements that expand or contract all coordinates of the particles as well as the total size of the system. The rescaling is accepted or rejected depending on the energy change it involves. The contraction-expansion procedure is made independently for the three spatial coordinates, and the maximum ratio between the size of the system in different directions is limited to 1.2.

A subtle but important technical change was introduced in the simulation procedure to be able to equilibrate the volume in the low temperature region. Let us think for instance of the $T = 0$ case. If we increase P , as soon as two particles are at a distance r_0 from each other, the total volume gets stuck in the simulation because (due to the scheme adopted for doing volume changes) the volume can be reduced further only if a global contraction of all coordinates reduces the energy. But this contraction would bring the two particles (which are already at a distance r_0) at a distance lower than r_0 , then formally to a state of infinite energy, and so the trial movement is rejected. To avoid this problem we relax a bit the rigid hard core at r_0 , replacing it by a new linear ramp between $r = 0$ and $r = r_0$ of the form $U(r) = \varepsilon_0[50(1 - r/r_0) + 1]$. The last term is included in order to match smoothly the potential for $r > r_0$. This modification was seen not to modify the behavior of the system, it just provides a convenient way of reaching the equilibrium values of the volume within a reasonable computing time in the low temperature regime.

The property of the potential that renders it interesting for our problem is that depending on the external force acting on them, two particles prefer to be at distance r_0 or r_1 from each other, and the effect of this simple fact on the phase diagram is dramatic.²⁰ Already in the original papers about this potential,¹⁸ it was realized that in fact the competition between configurations with particles at distances r_0 and r_1 may produce the appearance of polymorphism in the system. More precisely, in 1D the system may exhibit many liquid phases when $\gamma \neq 0$, with sharp transitions between them. In 3D these transitions occur within the solid region of the phase diagram, and it was suggested that they may still be observable as isostructural transitions of the solid.^{18,21} In this connection we want to emphasize the following two points: i) isostructural transitions within the solid phase for this kind of potentials are usually preempted by the appearance of new intervening solid phases of different symmetry; ii) polymorphism of the liquid state as observed in the 1D system also appears in 3D samples, but now

in the supercooled liquid state, and is the responsible for the existence of the second critical point. We address these two points in the next two sections.

III. CRYSTALLINE CONFIGURATIONS AT $T = 0$

Multiple crystalline structures for our potential arise from the competition between expanded and contracted structures. At $T = 0$ the preferred configuration of the system will be the one that minimizes the enthalpy $h \equiv e + Pv$. At low P the best way of minimizing h is first to minimize e , and then v . This is achieved in a close packed structure with first neighbors distance equal to r_1 . At very large P , in order to minimize h it is energetically more convenient to minimize v , and the structure becomes again a close packed one with first neighbors distance equal to r_0 . However, in the range in which these two configurations have approximately the same enthalpy, there are others which are more stable, having pairs of neighbor particles both at distances r_0 and r_1 . For our potential $U(r)$ (and also for more general potentials) the existence of other stable configurations can be demonstrated quite generally.^{22,23} However, to tell safely which is the structure of lowest enthalpy for each P is a problem for which a closed solution is not known. The usual approach is to compare the enthalpies of structures proposed beforehand, using simulated annealing techniques to guess the possible structures. We refer to [22,23] for a detailed discussion of the two-dimensional case, and also for discussions on the necessary conditions on the potential for different structures to appear.

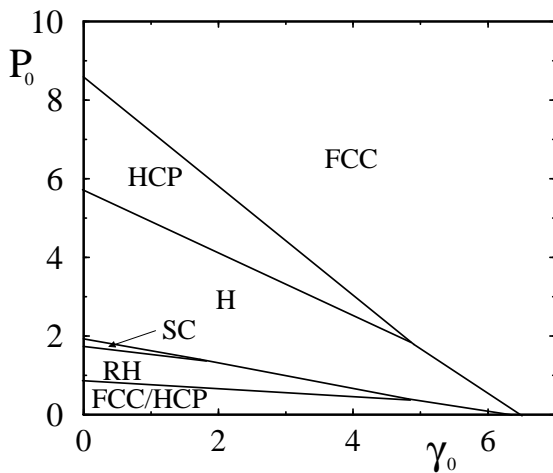


FIG. 1. Crystalline structures of highest stability for different values of P and γ , for $r_1/r_0 = 1.75$ and $T = 0$ (adiimensional values of P and γ are defined as $P_0 \equiv Pr_0^3\epsilon_0^{-1}$, and $\gamma_0 \equiv \gamma\epsilon_0^{-1}r_0^{-3}$). The search was performed among structures of the cubic (simple (labeled SC), face centered (FCC), and body centered), tetragonal (simple, and body centered), rhombohedral (RH), and hexagonal (simple (H), and close packed (HCP)) crystalline systems, with only one particle per unit cell (except for the HCP structure). However, other more complex structures cannot be ruled out.

Here we show only in Figure 1 the result of comparing (for $r_1/r_0 = 1.75$) the enthalpies of particles arranged in Bravais lattices corresponding to cubic, tetragonal, rhombohedral, and hexagonal systems as a function of P and γ . The structures searched are those that can be defined by no more than two parameters (that fix the form and size of the Bravais lattice). All of them were supposed to have only one particle per unit cell, except for HCP (which has two), that was included due to its known stability. We find five different crystalline configurations as a function of P . Note also how the increasing of the van der Waals attraction moves all the borders between structures to lower pressures, since those that are stable at higher P are always more compact, and thus become more stable in the presence of the van der Waals term. It must be kept in mind that there may be other configurations (corresponding to other crystalline systems, or with more complex unit cells) with lower enthalpy. In fact, they are likely to occur, as for instance in the 2D case crystalline structures with up to five particles per unit cell appear.^{22,23} Only a thorough numerical work can determine all possible structures.

IV. PROPERTIES IN THE FLUID AND SUPERCOOLED REGIONS

In the previous section we saw that at $T = 0$ there is a sequence of solid phases interpolating between the lowest density and highest density ones. At each transition (as P is increased) a finite fraction of particles that were at distance r_1 from each other passes to be at distance r_0 . Each of these rearrangements involves a change of symmetry, and thus the appearance of a new crystalline structure. The picture is different in the metastable, disordered sheet of the phase diagram. At very low pressures the particles behave as hard spheres with radius $r_1/2$. Hard spheres are known to have a maximum density of random packing, corresponding to a volume per particle v_1 than in our case is $v_1 \simeq 0.808r_1^3$. Being the densest disordered structure possible for hard spheres, this is also the thermodynamically stable amorphous configuration of the system when $T = 0$, namely, the one which minimizes the enthalpy. When $P \rightarrow \infty$ the linear ramp of $U(r)$ is irrelevant to calculate the free energy, and the thermodynamically stable configuration is again a random packing of spheres, now with radius $r_0/2$. As in the

crystalline case, the nearest neighbor distance between particles must collapse from r_1 to r_0 as a function of P . The crucial question is whether this collapse is discontinuous at some well defined P (or even if there are more than one transitions at different values of P) or if it is just a smooth crossover. We address the issue in the following two subsections, first analytically (when $r_1/r_0 \rightarrow \infty$) and then numerically, but let us quote briefly the answer to this question in advance. For the case of no van der Waals attraction the behavior of the specific volume v as a function of P is smooth at any finite temperature. But there is a range of pressures in which $\frac{\partial v}{\partial P}$ is anomalously large. This fact is enough for the van der Waals interaction to produce (if sufficiently strong) the appearance of a metastable critical point and a line of first order transitions between two disordered structures with a finite difference in density.

A. The limit $r_1/r_0 \rightarrow \infty$

We will start by considering only the repulsive part of the potential (i.e., $\gamma = 0$). As we already said, at very low pressures the particles behave as hard spheres with radius $r_1/2$. At $T = 0$ the enthalpy per particle of this configuration is $h = Pv_1$. This is the thermodynamically stable state upon increasing P up to the point where it is energetically more convenient to overlap neighbor particles in pairs. The structure will now be similar to the low pressure one, but with two particles overlapped on each position (see a sketch of this fact in Figure 2). The enthalpy of this configuration is $h' = Pv_1/2 + \varepsilon_0/2$, since now the total volume of the system is reduced in a factor 2, and an energy ε_0 must be counted for each pair of particles. The pressure at which $h = h'$ determines the transition pressure $P_{TR} = \varepsilon_0/v_1$. Close to the point $(P_{TR}, T = 0)$ of the phase diagram, we can calculate approximately the free energy of the system in the following way. Let us suppose we have N particles, n of them in non overlapped positions and n' pairs of overlapped particles ($N = n + 2n'$). The configurational free energy of the system may be written as (higher than double overlaps that will occur at higher pressures are dismissed)

$$F = [Pv' - Ts^{HS}(v')](n + n') + \varepsilon_0 n' - Ts^I \quad (1)$$

where $v' \equiv V/(n + n')$ [note that v' is not the specific volume, which instead is given by $v = V/(n + 2n')$], $s^{HS}(v')$ is the entropy per particle of hard spheres with radius r_1 on the metastable sheet, and s^I is the configurational entropy for choosing which particles will be in pairs, and which ones will be singled $\left[s^I = k_B \ln \binom{n + n'}{n'} \right]$. Using v' and n' as independent variables for minimizing F we obtain the equations

$$\frac{P}{T} = \frac{\partial s^{HS}(\tilde{v}')}{\partial \tilde{v}'} \quad (2)$$

$$\frac{P\tilde{v}'}{T} - s^{HS}(\tilde{v}') = \frac{\varepsilon_0}{T} - k_B \ln \frac{(1 - 2n'/N)^2}{(1 - n'/N)n'/N} \quad (3)$$

(we use \tilde{v}' in this case with $\gamma = 0$, to distinguish from the $\gamma \neq 0$ case).

The first one is the equation of state of hard spheres in the metastable region. We will use for it the following expression provided by Speedy²⁴

$$\frac{P}{T} = \frac{2.65k_B}{\tilde{v}' - v_1} \quad (4)$$

For given values of P and T , \tilde{v}' is determined from this equation, and the value obtained is used to determine n' from (3).²⁵

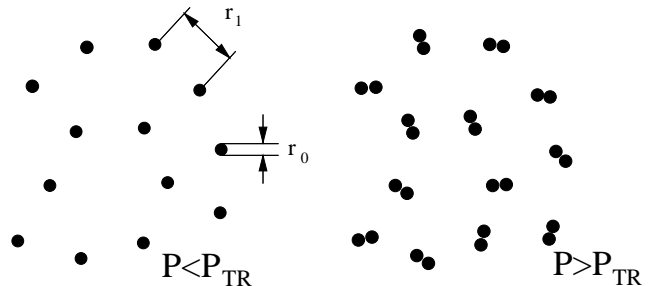


FIG. 2. Sketch of two dimensional configurations of particles in a glassy state at $T = 0$ for r_1/r_0 large, although finite, below and above the transition pressure P_{TR} . Drawings were made so as to emphasize that for $P > P_{TR}$ (b) the structure is similar to that at $P < P_{TR}$ (a) but with two particles per site, instead of one (this fact is strictly valid if $r_1/r_0 \rightarrow \infty$). The density of the system is roughly twice in (b) than in (a). The energy per particle is 0 in (a) and $\varepsilon_0/2$ in (b).

The volume per particle of the system is $\tilde{v} \equiv V/N = \tilde{v}'(n + n')/N$. Although \tilde{v}' has a behavior on P and T that is the same as for hard spheres, the $(n + n')$ factor (that takes the value N when $T = 0$, $P < P_{TR}$, and $N/2$ when $T = 0$, $P > P_{TR}$) makes the behavior of v on T and P be non trivial. We see the surface $\tilde{v}(P, T)$ that is obtained from equations (2), (3), and (4) in Fig. 3. At $T = 0$ we obtain the expected result, with $\tilde{v}(P, T = 0)$ passing from v_1 to $v_1/2$ at the transition pressure P_{TR} . But at any finite T the entropy transforms this jump in a smooth crossover. The point $P = P_{TR}$, $T = 0$ is for this system the metastable critical point.

The inclusion of a finite long range attraction through a non zero γ produces the critical point to move into the $T > 0$ region. The mechanism is identical to the one that produces the appearance of the usual liquid-gas coexistence curve. We must replace P by $P + \gamma/v^2$ in expressions (2), (3), and (4) to take account of the van der Waals attraction. A singularity in $v(P)$ at a finite temperature exists if $\partial v/\partial P$ becomes negative (this is the signature of a van der Waals loop, and thus of a first order transition). Since

$$v(P) = \tilde{v}(P + \gamma/v^2), \quad (5)$$

we can calculate $\partial v/\partial P$ as

$$\frac{\partial v}{\partial P} = \frac{\frac{\partial \tilde{v}(x)}{\partial x}}{1 + \frac{2\gamma}{v^3} \frac{\partial \tilde{v}(x)}{\partial x}} \bigg|_{x=P+\gamma/v^2}. \quad (6)$$

We see that a singularity occurs if $\partial \tilde{v}(P)/\partial P$ is larger (in absolute value) than $\frac{v^3}{2\gamma}$. This always happens in our model close enough to P_{TR} , $T = 0$. In Figure 4 the function $v(P, T)$, calculated using the self consistency condition (5), with $\gamma_1 = 0.1$ ($\gamma_1 \equiv \gamma \varepsilon_0^{-1} r_1^{-3}$) is shown.

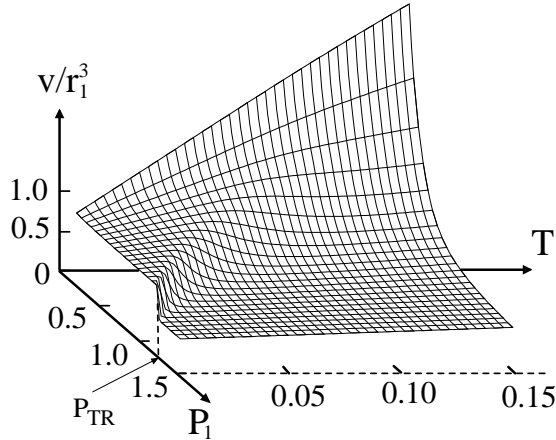


FIG. 3. The surface $v(P, T)$ for $\gamma_1 = 0$ ($\gamma_1 \equiv \gamma \varepsilon_0^{-1} r_1^{-3}$), when $r_1/r_0 \rightarrow \infty$. Only the $T = 0$ isotherm is singular, at $P = P_{TR}$ (T is measured in units of $k_B^{-1} \varepsilon_0$, $P_1 \equiv P r_1^3 \varepsilon_0^{-1}$).

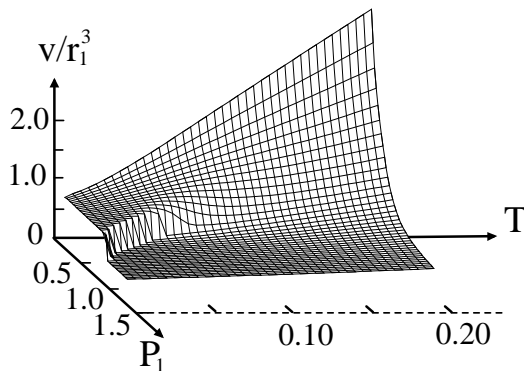


FIG. 4. Same as Figure (3), but with $\gamma_1 = 0.1$. Now a discontinuity exists for all $T \lesssim 0.37$.

The rapid change in v as a function of P close to the critical point is the responsible for the anomalous behavior of v and the isothermal compressibility $K_T \equiv -\frac{1}{v} \frac{\partial v}{\partial P}$.

We see the location in the P - T diagram of the extrema of v and K_T as a function of temperature in Figure 5. We also see in this figure the first order line that appears due to the van der Waals attraction, ending in the critical point C' , and also the two spinodal lines that mark the limit of metastability of the two phases on both sides of the first order line. Note that the singularity of the thermodynamic properties at the critical point manifests itself in anomalous properties (of v and K_T) that can be detected at higher temperatures.

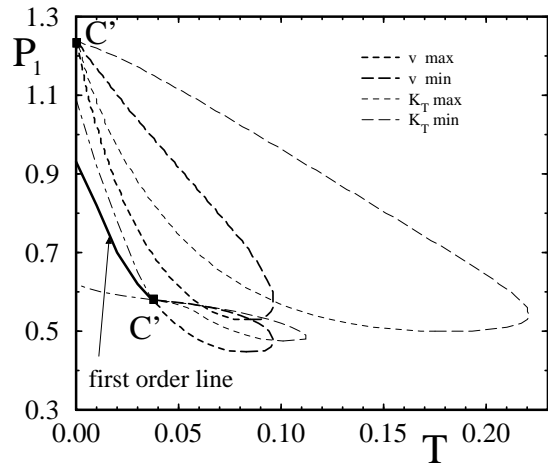


FIG. 5. The locus of extrema of v and K_T , calculated from the $v(P, T)$ function, for $\gamma_1 = 0$ (upper curves) and $\gamma_1 = 0.1$ (lower curves). For finite γ_1 a first order line ending in a critical point C' appears. The dashed-dotted lines are the spinodals of this first order transition.

The analytical treatment of the case $r_1/r_0 \rightarrow \infty$ provides insight into the appearance of the second critical point in the phase diagram of water. In fact, the anomalies in v and K_T exist even for exclusively repulsive potentials. It is the van der Waals attraction that brings the critical point to a finite temperature, in the same way that it is this attraction (or a more realistic finite range one) that generates the familiar liquid-gas coexistence line. Now we will see how much of this scenario remains for finite r_1/r_0 .

B. Numerical results for finite r_1/r_0

When r_1/r_0 is finite, no analytical calculation seems to be possible to tell the existence or not of the metastable critical point. But guided by the previous findings, we can more safely interpret the numerical results.

In Figure 6 we show the results of numerical simulations for $r_1/r_0 = 1.5$. Rapid runs (2000 steps per temperature) were made by decreasing the temperature at different values of P in a system of 197 particles. The rapid cooling allows to reach the supercooled states without

crystallization except in the continuous-dashed region.²⁶ The curves shown are averages over 20 different runs. Only the points in which the system did not crystallize and displays well reproducible values for the density are shown. In spite of this, since the runs were rapid and the low temperature states are highly viscous, we can rise some doubts about the final state reached for $T \rightarrow 0$. It might be that we are observing some frozen configuration typical of larger T . To answer this point we made runs at a low temperature ($T = 0.01$) increasing and decreasing pressure (Fig. 7). The results of this simulation show evident effects of hysteresis due to the glassiness of the states. This hysteresis was seen not to be greatly reduced by decreasing the rate of temperature change in a factor ten. But anyway the hysteresis path encloses the values of v obtained by decreasing T at fixed P (large symbols in Fig. 7), and we have also checked that the radial distribution functions are comparable in both cases. The finding of essentially the same results when we arrive from different paths in the P - T plane is an indication that in fact these are thermodynamic values.

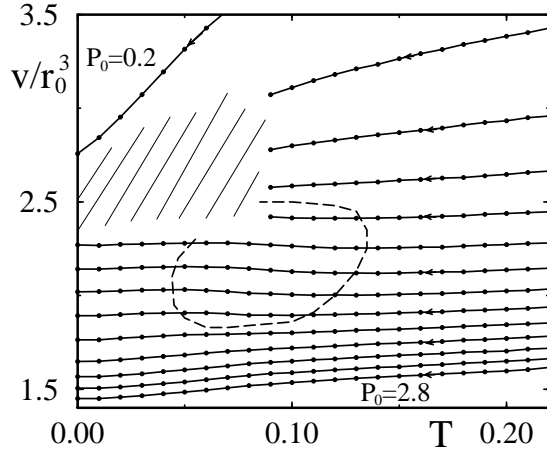


FIG. 6. Specific volume as a function of T for different values of P_0 ($P_0 = Pr_0^3 \varepsilon_0^{-1}$) from 0.2 to 2.8 in steps of 0.2, from the numerical simulations with $r_1/r_0 = 1.5$. Simulations were done reducing rapidly the temperature from the fluid state. Averages over 20 runs are shown. The continuous-dashed region corresponds to points where the system crystallization could not be avoided even in these rapid runs, and are thus not included. Within the region limited by the dashed line $\partial v/\partial T$ is negative.

There is no sign in Fig. 6 (in contrast to the $r_1/r_0 \rightarrow \infty$ case) of an abrupt jump in v as a function of P at $T = 0$, all that remains is a value of pressure with a maximum in $\partial v(P, T = 0)/\partial P$ (as is seen in Fig. 7, close to $P_0 = 2$). Around this value K_T has a maximum (as a function of T) at $T = 0$, whereas v has maxima and minima at finite temperature, as can be seen from Fig. 6 in the range $1.0 \lesssim P_0 \lesssim 1.8$ (on the dashed line). These facts

are sufficient for the van der Waals attraction to induce the appearance of a critical point, if γ is large enough. In fact, we find that for $\gamma_0 \equiv \gamma_0^{cr} \simeq 4.2$ a critical point enters the phase diagram at $T = 0$, $P_0 \simeq 0.65$. The location of the critical point as a function of γ can be determined from data as those of Fig. 6 by requiring that $\partial v/\partial P \rightarrow \infty$, and $\partial^2 v/\partial P^2 \rightarrow \infty$ calculated according to Eq. (6). We find in our case that for γ_0 slightly larger than γ_0^{cr} the critical point position can be estimated as

$$T^{cr} \simeq 0.07(\gamma_0 - 4.2) \quad (7)$$

$$P_0^{cr} \simeq 0.65 - 0.35(\gamma_0 - 4.2). \quad (8)$$

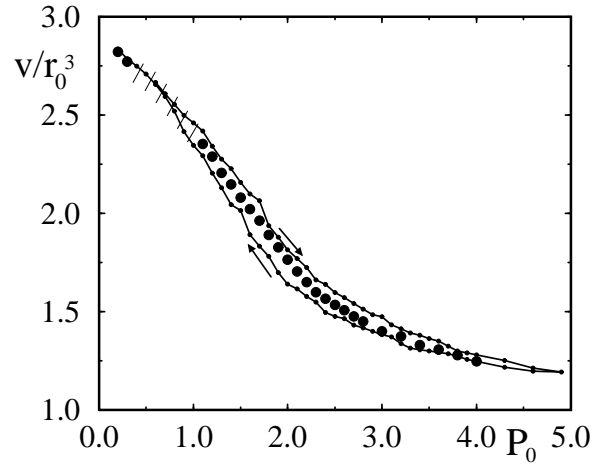


FIG. 7. Specific volume as a function of P at $T = 0$ from the simulations shown in Fig. 6 (large symbols) and from a single run at $T = 0.01$ (20000 steps per temperature) increasing and decreasing P (small symbols. The path of the simulation is indicated by the arrows). The dashed region contains no large symbols since here crystallization could not be avoided when reducing T . Note that the limiting values of v/r_0^3 at very high and low P are respectively 0.808 and 2.727.

The locus of the anomalies of v and K_T also move with γ . We note that if γ is such that the critical point exists, the line of K_T maxima necessarily ends at the critical point (since at the critical point $K_T \rightarrow \infty$). For the extrema of v this is not necessarily so, although it is known that the anomalies in K_T and v are thermodynamically related.¹³

V. CHARACTERISTICS OF MELTING

In this section we show results of numerical simulations that focus on the melting of the most expanded of the solid phases of our system²² (which is the equivalent of ice Ih in water). Figure 8 shows the specific volume v as a function of T for different values of P obtained in slow simulations decreasing and increasing T in

a system of 216 particles. The hysteresis upon heating and cooling embraces the position of the thermodynamic melting transition temperature. In all the range of P indicated in this figure, the system freezes into one and the same solid configuration, corresponding to a dense stacking of triangular planes, in which each particle has twelve nearest neighbors at distance r_1 (the dispersion in the limiting value of v when $T \rightarrow 0$ is due to a few defects that remain in the solid structure). Upon increasing T , v increases for $P_0 \lesssim 0.95$ (which is of course the standard behavior), but decreases for larger P_0 . This decrease is driven by the possibility of particles of being at distances smaller than r_1 from each other. Depending on P , the tendency of particles to become closer (gaining energy from the Pv term) may be higher than the entropic tendency to increase v . In the same way, at the lowest pressures, the solid melts by increasing its volume, whereas at the largest pressures shown in Fig. 8 it melts by reducing its volume. This is consistent with the form of the solid-liquid border in the P - T plane that is seen in Figure 9, which has positive derivative at low P , but has negative derivative at larger P .

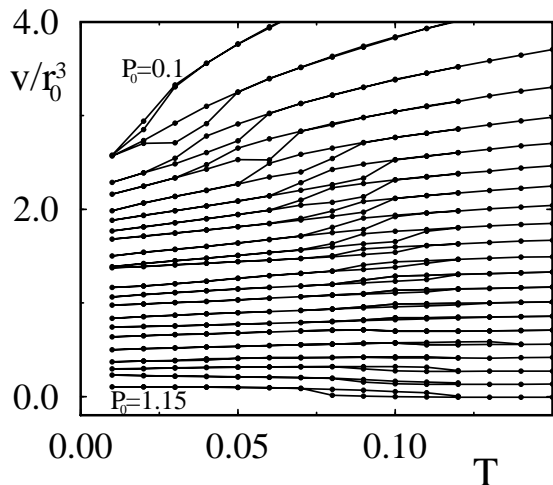


FIG. 8. The specific volume v as a function of T for different values of P_0 , from 0.1 to 1.15, in steps of 0.05 for a system of 216 particles. Each curve was vertically displaced by a term $-2P_0$ to allow a better visualization. Hysteresis is the result of successive cooling and heating. Note the normal melting at low P_0 , and the anomalous one for $P_0 \gtrsim 0.95$.

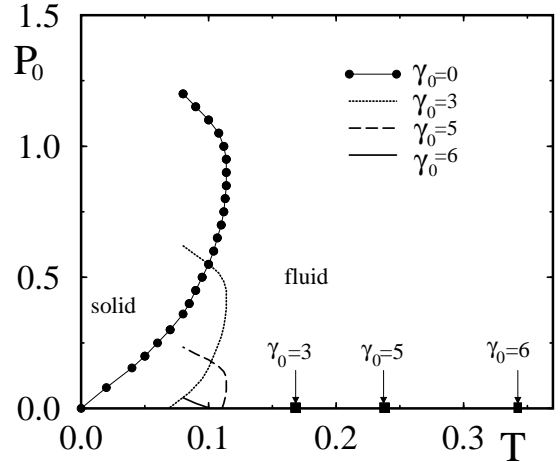


FIG. 9. The melting line of the lowest pressure solid structure, for $\gamma_0 = 0, 3, 5$, and 6 . There is also a liquid-gas coexistence line for all $\gamma_0 \neq 0$ that in the scale of the figure cannot be distinguished from the $P_0 = 0$ axis. This line ends in the critical point indicated for each case by a square.

In the same Figure 9 we see the modification of the phase diagram when we consider the van der Waals attraction. Any finite value of γ makes a liquid-gas first order line appear.¹⁹ In the scale of Fig. 9 this critical line cannot be distinguished from the $P = 0$ axis, only the critical temperature is indicated. In addition, the whole solid-fluid coexistence line basically moves down with γ_0 . If $\gamma_0 \lesssim 5.5$ the triple point that is defined is ‘standard’, in the sense that the slope of the solid-liquid coexistence line is positive at the triple point. For larger γ_0 the triple point is ‘anomalous’ (the slope of the solid-liquid coexistence line is negative).

VI. SUMMARY AND CONCLUSIONS

We studied the phase diagram of a model of spherical particles with pairwise interactions, consistent of a hard core at a distance r_0 plus a repulsive linear shoulder that extends up to distance r_1 . This potential favors the particles to be in one or the other (depending on P) of the two different equilibrium distances r_0 and r_1 . On top of that, a long range van der Waals attraction was also included.

The solid phase of the system exhibits polymorphism. Namely, there are different sectors of the P - T phase diagram in which the crystalline structure of the system is different. This behavior is observed even in the case of non attractive part in the potential (i.e., $\gamma = 0$).

The fluid phase part of the phase diagram has the following characteristics. At low pressures particles prefer to be at distances $\sim r_1$ from each other, whereas at high pressures the typical distance is r_0 ($< r_1$). This implies a crossover region of P with an anomalously large isother-

mal compressibility K_T . When we include the van der Waals attraction ($\gamma \neq 0$) the anomaly in K_T may become (if γ is sufficiently large) a first order transition line (similar to the liquid-gas coexistence line). This first order line starts from a finite P at $T = 0$, and ends in a critical point at finite T and P . From this point the line of K_T maxima continues towards larger values of T . There are also anomalies in the density of the system, which has extrema in a locus that, whereas it does not necessarily touch the critical point, appears in the region that is influenced by the existence of it.

For $\gamma = 0$, the melting line of the most expanded solid structure in the P - T plane has positive derivative at low pressures, but is reentrant at higher P . This reentrant behavior is associated (through the Clausius-Clapeyron equation) to a melting with density increasing. When the van der Waals attraction is included, a liquid-gas first order line appears, that ends in a critical point as usual. This liquid-gas line defines a triple point where it meets the fluid-solid line. For small γ the slope of the solid-liquid line at the triple point is positive, but it becomes negative if γ is large enough.

Our model, although very simple, has many of the properties that characterize water as an anomalous fluid, and gives insight into the properties of real water. Actually, the simplicity of the model allows to single out the crucial characteristic that produces all the anomalies, without the complications introduced by non-spherical interactions and cooperative hydrogen bonding in real water. This characteristic is the existence in the interatomic potential of two different equilibrium distances for the particles. From all our results it is difficult to elude the claim that there must be an effective description of the interaction in water in which two different distances compete as being the most stable one. In fact, it would be even more daring to say that all the similarities we found are accidental. Although there is evidence favoring this view,^{3,27,28} the complications added by the peculiarities of water molecules has made this point very disputed.²⁹

Among all anomalous properties of water, the existence of the second critical point is the one that is not fully proven to occur, and also the one that has been most elusive to address numerically in previous studies. Our model shows that its existence is a consequence of the effect of the attractive part of the potential on a system that (due to peculiarities of the interaction) possesses anomalously large values of K_T at some pressure. At this point experimental evidence about the existence of two amorphous phases (LDA and HDA) that transform reversibly into each other seems crucial to indicate that in water, the attraction between molecules is strong enough to bring the second critical point into existence.

From a more fundamental point of view, we note that our model has essentially two free parameters, the ratio between equilibrium distances r_1/r_0 and the strength of the van der Waals attraction γ . Other characteristics, as if the ramp between r_0 and r_1 is linear or not, are

only marginal for the phase diagram that is obtained.²² An important result of our study is the fact that these two parameters determine the phase behavior of the fluid phase both in the zone where the fluid is stable, and also in the deeply supercooled region. If water admits a similar effective representation in term of two parameters,³⁰ then these could be extracted from fitting experimental data in the high temperature region, and then used, relying on our model, to predict the supercooled part of the phase diagram, in particular the existence and location of the second critical point. This means that the present model may even be of quantitative importance. Work on this direction is under way.

-
- ¹ *Water, a Comprehensive Treatise*, edited by F. Franks (Plenum, New York, 1972).
 - ² C. A. Angell in Ref. [1], Vol. 7.
 - ³ O. Mishima and H. E. Stanley, *Nature (London)* **396**, 329 (1998).
 - ⁴ P. G. Debenedetti, *Metastable Liquids* (Princeton University Press, Princeton, 1997).
 - ⁵ C. A. Angell, *Science* **267**, 1924 (1995).
 - ⁶ R. J. Speedy, *Nature (London)* **380**, 289 (1996).
 - ⁷ R. J. Speedy and C. A. Angell, *J. Chem. Phys.* **65**, 851 (1976).
 - ⁸ O. Mishima, L. D. Calvert, and E. Whalley, *Nature (London)* **310**, 393 (1984); **314**, 76 (1995); O. Mishima, K. Takemura, and K. Aoki, *Science* **254**, 406 (1991); O. Mishima, *J. Chem. Phys.* **100**, 5910 (1994).
 - ⁹ R. S. Smith and B. D. Kay, *Nature (London)* **398**, 788 (1999); R. J. Speedy, P. G. Debenedetti, R. C. Smith, C. Huang, and B. D. Kay, *J. Chem. Phys.* **105**, 240 (1996).
 - ¹⁰ P. H. Poole, F. Sciortino, U. Essmann, and H. E. Stanley, *Nature (London)* **360**, 324 (1992).
 - ¹¹ P. H. Poole, F. Sciortino, T. Grande, H. E. Stanley, and C. A. Angell, *Phys. Rev. Lett.* **73**, 1632 (1994).
 - ¹² H. Tanaka, *Phys. Rev. Lett.* **80**, 5750 (1998).
 - ¹³ S. Sastry, P. Debenedetti, F. Sciortino, and H. E. Stanley, *Phys. Rev. E* **53**, 6144 (1996).
 - ¹⁴ H. E. Stanley and J. Teixeira, *J. Chem. Phys.* **73**, 3404 (1980).
 - ¹⁵ H. E. Stanley *et al.*, *Physica (Amsterdam)* **A205**, 122 (1994); H. E. Stanley *et al.*, *Physica (Amsterdam)* **236A**, 19 (1997); F. Sciortino, P. H. Poole, U. Essmann, and H. E. Stanley, *Phys. Rev. E* **55**, 727 (1997).
 - ¹⁶ H. Tanaka, *Nature (London)* **380**, 328 (1996).
 - ¹⁷ C. J. Roberts, A. Z. Panagiotopoulos, and P. G. Debenedetti, *Phys. Rev. Lett.* **77**, 4386 (1996); E. G. Ponyatovskii, V. V. Sinitsyn, and T. A. Pozdnyakova, *JETP Lett.* **60**, 360 (1994); A. C. Mitus and A. Z. Patashinskii, *Acta Phys. Pol.* **74**, 779 (1988).
 - ¹⁸ P. C. Hemmer, and G. Stell, *Phys. Rev. Lett.* **24**, 1284 (1970); G. Stell and P. C. Hemmer, *J. Chem. Phys.* **56**, 4274 (1972).

- ¹⁹ P. C. Hemmer and J. L. Lebowitz, in *Phase Transitions and Critical Phenomena*, edited by C. Domb and M. S. Lebowitz (Academic, London, 1976), Vol.5.
- ²⁰ M. R. Sadr-Lahijany, A. Scala, S. V. Buldyrev, and H. E. Stanley, Phys. Rev. Lett. **81**, 4895 (1998).
- ²¹ J.M. Kincaid, G. Stell, and E. Goldmark, J. Chem. Phys. **65**, 2172 (1976).
- ²² E. A. Jagla, Phys. Rev. E **58**, 1478 (1998).
- ²³ E. A. Jagla, J. Chem. Phys. **110**, 451 (1999).
- ²⁴ R. J. Speedy, Molec. Phys. **83**, 591 (1994); R. J. Speedy, J. Chem. Phys. **100**, 6684 (1994).
- ²⁵ In order to use Eq. (3), it is still necessary to know the integration constant when we determine s_{HS} from (4) and (2). This constant is physically related to the fact that we have divided the total entropy in a vibrational (s^{HS}) and a combinatorial (s^I) part. Since a precise determination of this constant is difficult, and we pursue a qualitative description of the phase diagram, we took this constant to be zero, having verified that finite values do not change the qualitative characteristics of the results.
- ²⁶ Reaching of metastable configuration without crystallization in this system is rather easy because of the nature of the interaction potential, that allows for the existence of competing structures, from which frustration and disorder appears [see H. Tanaka, J. Phys. C **10**, L207 (1998)].
- ²⁷ C. H. Cho, S. Singh, and W. Robinson, Phys. Rev. Lett. **76**, 1651 (1996).
- ²⁸ M. Campolat *et al.*, Chem. Phys. Lett **294**, 9 (1998).
- ²⁹ E. Velasco, L. Mederos, and G. Navascués, Phys. Rev. Lett. **79**, 179 (1997); C. H. Cho, S. Singh, and W. Robinson, *ibid.* **79**, 180 (1997).
- ³⁰ In fact, fitting of properties of water in the stable and metastable regime with expressions derived from a Landau-type theory with only one free parameter is remarkably good (see Ref. [12]).